

# Determination of energy transfer and upconversion constants for $\text{Yb}^{3+}/\text{Er}^{3+}$ codoped phosphate glass

Suya Feng (冯素雅)<sup>1\*</sup>, Fei Luan (栾飞)<sup>1</sup>, Shunguang Li (李顺光)<sup>1</sup>, Li Chen (陈力)<sup>1</sup>, Biao Wang (王标)<sup>1</sup>, Wei Chen (陈伟)<sup>1</sup>, Lili Hu (胡丽丽)<sup>1</sup>, Y. Guyot<sup>2</sup>, and G. Boulon<sup>2</sup>

<sup>1</sup>Key Laboratory of Material for High Power Lasers, Shanghai Institute of Optics and Fine Mechanics, Chinese Academy of Sciences, Shanghai 201800, China

<sup>2</sup>Physical Chemistry of Luminescent Materials, University of Lyon, Villeurbanne 69622, France

\*E-mail: suyafeng21@yahoo.com.cn

Received April 2, 2009

The energy transfer and cooperation upconversion processes are investigated in  $\text{Yb}^{3+}/\text{Er}^{3+}$  codoped phosphate glass. Based on the measured curves of output power versus incident power, the laser and spectroscopic parameters of the glass are fitted and analyzed. We focus on the resonant energy transfer constant  $k$  from  $\text{Yb}^{3+}$  to  $\text{Er}^{3+}$  as well as the cooperation upconversion coefficient  $C_{\text{up}}$  from  ${}^4\text{I}_{13/2}$  of  $\text{Er}^{3+}$ . The fitted  $k$  and  $C_{\text{up}}$  can give almost the same results for different thicknesses of glass disk with the same doping concentrations. The determination of these parameters is helpful for the development of  $\text{Yb}^{3+}/\text{Er}^{3+}$  codoped laser glass.

OCIS codes: 140.3500, 160.3380, 140.2020, 140.3580.

doi: 10.3788/COL20100802.0190.

$\text{Yb}^{3+}/\text{Er}^{3+}$  codoped glass lasing at 1.5  $\mu\text{m}$  has been studied extensively in recent years owing to their use for eye-safe range application, as well as for optical communication<sup>[1-4]</sup>. For a  $\text{Yb}^{3+}/\text{Er}^{3+}$  codoped system, the large absorption cross section of  $\text{Yb}^{3+}$  ( ${}^4\text{F}_{7/2}$ ) and effective energy transfer (ET) mechanism of  $\text{Yb}^{3+}$  ( ${}^4\text{F}_{5/2}$ ) to  $\text{Er}^{3+}$  ( ${}^4\text{I}_{15/2}$ ) can enhance the absorption of pump energy strongly. High phonon energy of phosphate glass enhances the multi-phonon decay (MPD) probability from  $\text{Er}^{3+}$   ${}^4\text{I}_{11/2}$  to  ${}^4\text{I}_{13/2}$ , which minimizes the back ET from  $\text{Er}^{3+}$  to  $\text{Yb}^{3+}$ . If the back ET is not considered as a major factor, the effective ET from  $\text{Yb}^{3+}$  to  $\text{Er}^{3+}$  should be the combined effect of ET and MPD. The upconversion (UC) processes are UC<sub>1</sub>:  $\text{Yb}^{3+}$  ( ${}^2\text{F}_{5/2}$ ) +  $\text{Er}^{3+}$  ( ${}^4\text{I}_{11/2}$ )  $\rightarrow$   $\text{Yb}^{3+}$  ( ${}^2\text{F}_{7/2}$ ) +  $\text{Er}^{3+}$  ( ${}^4\text{F}_{7/2}$ ); UC<sub>2</sub>:  $\text{Yb}^{3+}$  ( ${}^2\text{F}_{5/2}$ ) +  $\text{Er}^{3+}$  ( ${}^4\text{I}_{13/2}$ )  $\rightarrow$   $\text{Yb}^{3+}$  ( ${}^2\text{F}_{7/2}$ ) +  $\text{Er}^{3+}$  ( ${}^4\text{F}_{9/2}$ ); UC<sub>3</sub>:  $\text{Er}^{3+}$  ( ${}^4\text{I}_{13/2}$ ) +  $\text{Er}^{3+}$  ( ${}^4\text{I}_{13/2}$ )  $\rightarrow$   $\text{Er}^{3+}$  ( ${}^4\text{I}_{15/2}$ ) +  $\text{Er}^{3+}$  ( ${}^4\text{I}_{9/2}$ ). All upconversion processes dissipate the population of  $\text{Er}^{3+}$   ${}^4\text{I}_{13/2}$ , and some processes are the main loss channels. However, with only considering ET and UC<sub>3</sub>, corresponding parameters are still hard to be measured directly. Taccheo *et al.* measured the parameters of ET and UC<sub>3</sub> based on the suitable fit of the luminescence decay of the  $\text{Er}^{3+}$   ${}^4\text{I}_{13/2}$  metastable level at 1.5  $\mu\text{m}$  as a function of time<sup>[5]</sup>. Laroche *et al.* predicted the ET efficiencies based on migration-assisted ET models by using absorption, excited-state absorption, and emission spectra for both  $\text{Er}^{3+}$  and  $\text{Yb}^{3+}$  ions<sup>[6]</sup>. Because of the difficulty to measure these parameters directly, the parameters are extracted from the literatures in continuous-wave (CW) end-pump ytterbium-erbium laser models, even if the glass host and doping concentration are different<sup>[7,8]</sup>. It reduces the accuracy of judging the properties of material and delays the development of laser materials.

In this letter, we investigate the energy transfer constant  $k$  from  $\text{Yb}^{3+}$  to  $\text{Er}^{3+}$  and the cooperative upconver-

sion coefficient  $C_{\text{up}}$  of the  $\text{Er}^{3+}$   ${}^4\text{I}_{13/2}$  level in  $\text{Yb}^{3+}/\text{Er}^{3+}$  phosphate glass. It is well known that the increase of  $k$  can improve the utilization of pump energy and the energy conversion efficiency. UC processes would generate extra heat in glass because of the multi-phonon radiation and this may induce strong thermal stress, and thermal lensing in material. Therefore, one of our goals is to optimize the laser glass material by maximizing  $k$  and minimizing  $C_{\text{up}}$ .

The experimental configuration used for our diode-pumped laser is illustrated in Fig. 1. The resonator design is a standard plane-concave configuration with a total reflecting mirror coated with high-reflection film (reflectivity ( $R$ )=99.9%) at 1535 nm, which is validated by transmittance spectrum, and a 50-mm radius-of-curvature output spherical mirror coated with antireflection film (transmissivity ( $T$ )=1%) which is also validated. The total cavity length is 10 mm. We fabricated the active material and polished it into plane-plane phosphate glass block. The doping concentration of  $\text{Yb}^{3+}$  and  $\text{Er}^{3+}$  are  $1.64 \times 10^{21}$  and  $2.54 \times 10^{19}$   $\text{cm}^{-3}$ , respectively. The thicknesses of the laser medium block  $l_G$  are 0.5 and 1.0 mm. The glass block is cooled by a copper heat sink. The diode laser (HLU15F200-980, Liom, Germany) provides the input power on the active material centered at the wavelength of 980 nm, and the dimension focused on the active material is about 200  $\mu\text{m}$ . The precision of powermeter used in the experiment is 10  $\mu\text{W}$ . The whole

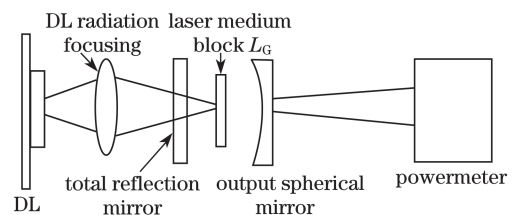


Fig. 1. Schematic of the experimental setup. DL: diode laser.

setup is fixed and the parallelism of the optical axis is calibrated by far-field He-Ne laser. The power casted on the active material is measured at the focus of the focusing system to decrease the influence of total reflecting mirror, and the unabsorbed pump light transmitting from the output spherical mirror is deducted from the detected output power.

Figure 2 shows typical curves of the output power versus the incident pump power obtained with the general cavity configuration in Fig. 1. Figure 2(a) shows the output power versus the incident power with the glass thickness of 0.5 mm. The maximal output power is 20.3 mW when the pump power is 315 mW. Figure 2(b) is that with the glass thickness of 1.0 mm, and the maximal output power is 17.9 mW when the pump power focused on the glass is 303 mW. The thresholds under these two conditions are about 29 and 59 mW, respectively. It is estimated that the intra-cavity loss for  $l_G=1.0$  mm is about double of that for  $l_G=0.5$  mm. The spot size of pump light is about  $200 \mu\text{m}$ , and the Rayleigh length is much longer than the thickness of glass used in our experiment, so we assume that the spot size in the glass is constant at different thickness. Actually, this means that we can use the same rate equations with different thickness to describe the laser characteristics. From Fig. 2, we can see that a good linear relation for both thicknesses is kept between the output power and the incident pump power. For a laser system, only when the laser modes completely oscillate, and the heat loading in the active material is moved effectively by a cooler, the curve of the output power versus the incident pump power can be linear. When the incident power is near the threshold, under which the laser modes cannot oscillate completely, the efficiency increases with the increase of incident power until it equals the slope of line. Meanwhile, when the incident power is too high, the stability of cavity will be distorted because of the thermal lens effect induced by the heat deposited in active material. This means that we should choose suitable pump power to avoid the phenomena discussed above. The rate equations of the  $\text{Er}^{3+}/\text{Yb}^{3+}$  codoped system (without considering the thermal effect) indicate that the relation of the incident pump power and the output power is linear for the fixed parameters. The slope efficiency and the threshold of the system are determined by the energy transfer and the upconversion parameters of the material and the loss of the cavity. So the linear curve

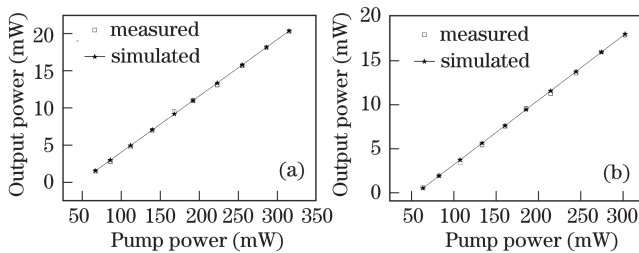


Fig. 2. Measured and simulated characteristics of the output power versus incident pump power. (a) The thickness is 0.5 mm, the parameters are  $k=3 \times 10^{-16} \text{ cm}^3/\text{s}$ ,  $C_{\text{up}}=1 \times 10^{-18} \text{ cm}^3/\text{s}$ ,  $L=0.00505$ ; (b) the thickness is 1.0 mm, the parameters are  $k=2.9 \times 10^{-16} \text{ cm}^3/\text{s}$ ,  $C_{\text{up}}=1 \times 10^{-18} \text{ cm}^3/\text{s}$ ,  $L=0.0115$ .

under suitable pump power could be used to fit the energy transfer and the upconversion parameters based on the model discussed in the next section. We also discuss the influence of the energy transfer and the upconversion parameters in the material and the loss in the cavity on the rate equation model.

A lot of work has been dedicated to the understanding of  $\text{Er}^{3+}/\text{Yb}^{3+}$  laser system, and the studies show that the main loss channels from the  $\text{Er}^{3+} {}^4\text{I}_{13/2}$  excited level are excited state absorption (ESA)<sup>[9]</sup> and cooperative UC<sup>[10]</sup> processes. It is well known that pumping at 980 nm is almost immune from ESA<sup>[11]</sup>, which is different from the other absorption bands. In phosphate glass, UC<sub>1</sub> process can be neglected due to the fast nonradiative relaxation from  $\text{Er}^{3+} {}^4\text{I}_{11/2}$  to  ${}^4\text{I}_{13/2}$  level. Based on the spectral and the quantum efficiency of the luminescence measured, the UC<sub>2</sub> process can also be neglected. So UC<sub>3</sub> process between two excited  $\text{Er}^{3+}$  ions, which promotes one ion to the  ${}^4\text{I}_{9/2}$  upper level while the other ion decays to the ground level, plays a major role in lowering the optical gain, particularly in highly  $\text{Er}^{3+}$  doped glass. Figure 3 shows the simplified scheme of the level and the energy transfer processes of  $\text{Yb}^{3+}/\text{Er}^{3+}$  codoping system, which is enough to describe our material. Through the discussion above, we can conclude that the output power is mainly decided by material parameters  $k$ ,  $C_{\text{up}}$ , and loss  $L$  in the cavity. The influence of these parameters can be shown in the rate equations which can describe the output characteristics of laser system. The rate equations for the  $\text{Yb}^{3+}/\text{Er}^{3+}$  codoped laser system are listed according to the energy levels

$$\frac{dN_1}{dt} = \frac{I_p \sigma_{\text{Yb}}}{h\nu_p} (1 - e^{-2\alpha l_G}) \frac{1}{\alpha l_G} + k N_{\text{Er}} N_4 (1 - N_1) - k N_{\text{Er}} N_1 N_2 - \frac{N_1}{\tau_{\text{Yb}}}, \quad (1)$$

$$\frac{dN_3}{dt} = -\frac{I_L}{h\nu_L} \sigma_{\text{Er}} (N_3 - N_2) + \frac{N_4}{\tau_4} - \frac{N_3}{\tau_{\text{Er}}} - 2C_{\text{up}} N_{\text{Er}} N_3^2, \quad (2)$$

$$\frac{dN_4}{dt} = k N_{\text{Yb}} N_1 N_2 - \frac{N_4}{\tau_4} - k N_{\text{Yb}} N_4 (1 - N_1), \quad (3)$$

$$\frac{dI_L}{dt} = \frac{I_L}{\tau_{\text{rt}}} [2\sigma_{\text{Er}} (N_3 - N_2) N_{\text{Er}} l_G - (L - \ln R)]. \quad (4)$$

In the above equations,  $N_1$  is the population of the  ${}^2\text{F}_{5/2}$  level of  $\text{Yb}^{3+}$  ion, and  $N_2$ ,  $N_3$ ,  $N_4$  present the populations

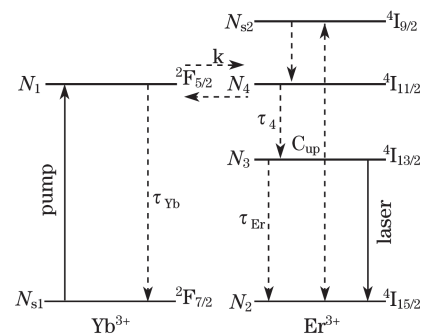


Fig. 3. Energy-level diagram for the  $\text{Yb}^{3+}/\text{Er}^{3+}$  system.  $N_{s1}$  presents the population of the  ${}^2\text{F}_{7/2}$  level of the  $\text{Yb}^{3+}$  ion,  $N_{s2}$  presents the population of  ${}^4\text{I}_{9/2}$  level of  $\text{Er}^{3+}$  ion.

of the  ${}^4I_{15/2}$  ground level,  ${}^4I_{13/2}$  metastable level, and  ${}^4I_{11/2}$  pump level of  $\text{Er}^{3+}$  ions, respectively. The concentrations of the  $\text{Yb}^{3+}$  and  $\text{Er}^{3+}$  are normalized, so  $N_1 + N_{s1} = 1$ ,  $N_2 + N_3 + N_4 + N_{s2} = 1$ .  $\nu_P$  and  $\nu_L$  are the pump frequency and laser frequency, respectively,  $\alpha$  is the absorption coefficient at the pump wavelength.  $\sigma_{Yb}$  is the absorption cross section of  $\text{Yb}^{3+}$  at pumping wavelength, and  $\sigma_{Er}$  is the stimulated emission cross section of  $\text{Er}^{3+}$  at laser wavelength.  $\tau_{Yb}$ ,  $\tau_{Er}$ , and  $\tau_4$  are the lifetimes of the  $\text{Yb}^{3+} {}^2F_{5/2}$ , the  $\text{Er}^{3+} {}^4I_{13/2}$ , and  ${}^4I_{11/2}$  levels, respectively, and  $\tau_{rt}$  is the cavity round trip time.  $k$  and  $C_{up}$  are the ET and UC coefficients, respectively.  $I_p$  is the pump photon flux, and it is the same for two glasses used in our experiment because of the pumping spot is generally a constant.  $I_L$  is the intra-cavity phonon power density.  $R$  is the reflectivity of output mirror.

We calculate the curves of output power versus incident power with  $N_{Yb} = 1.64 \times 10^{21} \text{ cm}^{-3}$ ,  $\tau_{Yb} = 1 \text{ ms}$ ,  $\sigma_{Yb} = 1.2 \times 10^{-20} \text{ cm}^2$ ,  $N_{Er} = 0.25 \times 10^{20} \text{ cm}^{-3}$ ,  $k = 3 \times 10^{-16} \text{ cm}^3/\text{s}$ ,  $C_{up} = 1 \times 10^{-18} \text{ cm}^3/\text{s}$ ,  $\tau_{Er} = 7.8 \text{ ms}$ ,  $\tau_4 = 2 \mu\text{s}$ ,  $\sigma_{Er} = 0.838 \times 10^{-20} \text{ cm}^2$ ,  $l_G = 0.5, 1.0 \text{ mm}$ , and  $R = 0.99$ . The results are shown in Fig. 2, which show that the relation between the output power and the incident power is linear. For fixed parameters, the slope efficiency and threshold are also fixed. The calculated results to estimate the influences from variant  $k$ ,  $C_{up}$ , and  $L$  on the laser characteristics are shown in Fig. 4.

Figure 4(a) are the calculated curves of the output power versus incident power, and the corresponding parameters are  $k = 1 \times 10^{-16}$ ,  $2 \times 10^{-16}$ , and  $3 \times 10^{-16} \text{ cm}^3/\text{s}$ , respectively.  $C_{up}$  and  $L$  remain to be a constant of  $1 \times 10^{-18} \text{ cm}^3/\text{s}$  and 0.0045. The slope efficiency and threshold are driven by  $k$  substantially, and the output power increases with the increase of  $k$ . In the rate equations,  $k \times N_1$  presents the effective pumping rate increasing with  $k$ . This means that the output power also increases with  $k$ . The parameter  $k$  is strongly dependent on the glass composition and concentration ratio of  $\text{Yb}^{3+}$  to  $\text{Er}^{3+}$ . For a fixed glass composition,  $k$  is mainly affected by the concentration of  $\text{Yb}^{3+}$ , because in the  $\text{Yb}^{3+}/\text{Er}^{3+}$  codoped system, the concentration of  $\text{Yb}^{3+}$  is normally 20–100 times higher than that of  $\text{Er}^{3+}$ . The higher doping concentration of  $\text{Yb}^{3+}$  can increase the absorption of pump light, and avoid the problem that the absorption cross section of  $\text{Er}^{3+}$  is small. Higher  $\text{Yb}^{3+}$  doping concentration can increase the energy transfer coefficient  $k$  from  $\text{Yb}^{3+}$  to  $\text{Er}^{3+}$ , and improve the effective pump rate by  $\text{Yb}^{3+}$  to  $\text{Er}^{3+}$  energy transfer. The  $\text{Yb}^{3+}$  to  $\text{Er}^{3+}$  energy transfer efficiency can reach 90%, but will fall to 80% under CW pumping and lasing condition because of the decrease of effective concentration of  $\text{Er}^{3+}$ [12]. So we should increase  $\text{Yb}^{3+}$  concentration to improve  $k$  at CW laser operation.

Figure 4(b) are the calculated influence of the cooperative UC coefficient  $C_{up}$  on the relation between the output power and the incident power, the corresponding parameters are  $C_{up} = 1 \times 10^{-18}$ ,  $2 \times 10^{-18}$ , and  $3 \times 10^{-18} \text{ cm}^3/\text{s}$ , respectively.  $k$  and  $L$  remain constant of  $3 \times 10^{-16} \text{ cm}^3/\text{s}$  and 0.0045, respectively. The slope efficiencies change slightly, and the threshold rises with the increase of  $C_{up}$ . In the equations,  $C_{up} \times N_3$  can be considered as a concentration-dependent nonradiative decay rate for  $\text{Er}^{3+}$  population of the excited  ${}^4I_{13/2}$  level, which means

that the higher  $C_{up}$  will lead to the lower output power. The energy stored in the upper level  ${}^4I_{9/2}$  relaxes through nonradiation and converts into heat loading in the glass. Some studies show that the thermal load induced by UC process is heavy[13,14]. If only considering with upconversion, it is suggested that the doping concentration of  $\text{Er}^{3+}$  should be low.

Figure 4(c) shows the influences of the intra-cavity loss  $L$  calculated by rate equations. The parameters used are  $L = 0.004, 0.005$ , and  $0.006$ , respectively.  $k$  and  $C_{up}$  remain to be  $3 \times 10^{-16}$  and  $1 \times 10^{-18} \text{ cm}^3/\text{s}$ . We can conclude from Fig. 4(c) that the slope efficiency and threshold are driven by  $L$  strongly. So decreasing the intra-cavity  $L$  can improve the slope efficiency and output power. Loss in the cavity is induced by the reabsorption and the scattering of the gain material[15]. Because the pump spot size just changes slightly in the gain material when the sample is thin[16], the loss in the cavity is decided by the length of gain material for a fixed condition[16].

We can conclude from the above discussion that the

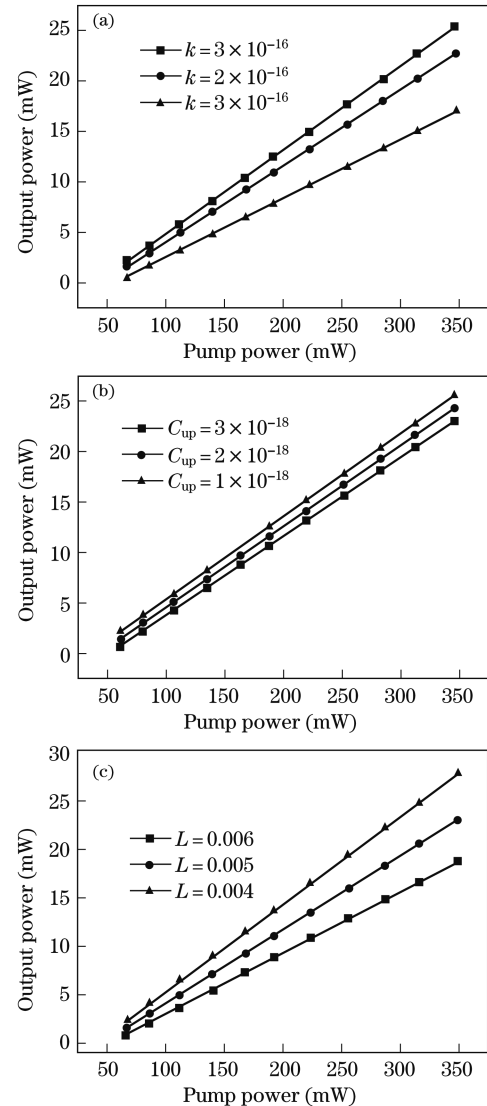


Fig. 4. Calculated effects of the parameters on the curves of the output power versus incident power for (a) the energy transfer coefficient  $k$ , (b) the cooperative upconversion coefficient  $C_{up}$ , and (c) the intra-cavity loss  $L$ .

slope efficiency and threshold are decided by  $k$ ,  $C_{\text{up}}$ , and  $L$  for our laser system. Namely the energy transfer coefficient  $k$ , the cooperation upconversion coefficient  $C_{\text{up}}$ , and the intra-cavity loss  $L$  in a phosphate glass laser system can be determined based on the experimental acquisition relationship between output and incident power, and then by a suitable fit of the experimental data which shows a considerable sensitivity to the fitting parameters. The fitting procedure relies on the numerical solution of the reasonable simplified rate equations built above. The fitting results for different thickness of gain material with the same doping concentration are shown in Fig. 2. For a certain concentration, the gain material parameters for different thickness are almost the same, and  $k$  and  $C_{\text{up}}$  are  $3 \pm 0.1 \times 10^{-16}$  and  $1 \pm 0.2 \times 10^{-18}$   $\text{cm}^3/\text{s}$ , respectively. It should be noted that the value of  $C_{\text{up}}$  is larger than that reported in Ref. [6]. The value of  $k$  turns to be smaller than that reported in Ref. [5], but larger than that in Ref. [5]. This could be explained by the difference of phosphate glass composition. The fitted intra-cavity losses are  $L_{0.5} = 0.005$  and  $L_{1.0} = 0.011$  for thickness of 0.5 and 1.0 mm, respectively.  $L_{1.0} \simeq 2L_{0.5}$  shows that the intra-cavity loss is proportional to the thickness of gain material. A slight difference is caused by the scattering of surfaces. The standard error of  $L$  is about 4% according to the measurement and calculation accuracy. These two fitted loss values are in good agreement with the analysis above. Therefore, the results of  $k$  and  $C_{\text{up}}$  we fit for our phosphate glass are reliable.

The  $\text{Yb}^{3+}$ -to- $\text{Er}^{3+}$  energy transfer coefficient  $k$  and cooperation upconversion coefficient  $C_{\text{up}}$  represent the characteristic of the gain materials for laser systems, so the determination of these parameters for different composition and doping concentration is very important. We investigate the parameters  $k$  and  $C_{\text{up}}$  of self-made phosphate glass with the concentrations of  $N_{\text{Yb}} = 1.64 \times 10^{21}$   $\text{cm}^{-3}$  and  $N_{\text{Er}} = 0.25 \times 10^{20}$   $\text{cm}^{-3}$ , respectively. For our phosphate glass, the parameter  $k$  of  $3 \times 10^{-16}$   $\text{cm}^3/\text{s}$  is different from those reported in other literatures. The value reported in Ref. [4] was  $1.8 \times 10^{-16}$   $\text{cm}^3/\text{s}$ . For the glass with  $k$  of  $5 \times 10^{-16}$   $\text{cm}^3/\text{s}$ , the output power at 315-mW pump power can improve 11% when the thickness of our glass is 0.5 mm. The value of  $C_{\text{up}}$  for our glass is larger than those reported, and this will result in heavier thermal load. The fitted parameters of  $k$  and  $C_{\text{up}}$  have the same order of magnitude with that reported in the literatures, but the values of these parameters are different because of the difference of glass composition and concentration ration. The values of parameters can be determinate by our method for a specific  $\text{Yb}^{3+}/\text{Er}^{3+}$  codoping phosphate glass, and this is helpful for optimizing glass.

In conclusion, we investigate both the  $\text{Yb}^{3+}$  to  $\text{Er}^{3+}$  energy transfer process and the cooperation upconversion process of  $\text{Er}^{3+}$   $^4\text{I}_{13/2}$  level in self-made  $\text{Yb}^{3+}/\text{Er}^{3+}$  codoped phosphate glass. Our study focuses on the ET and UC processes of glass. Based on the rational simplified rate equations of  $\text{Yb}^{3+}/\text{Er}^{3+}$  glass laser, the corresponding parameters of material and laser are fitted and analyzed by a precise measurement of the output–incident power curves of thin

glass disk. For our phosphate glass, when the concentrations of glass are  $N_{\text{Yb}} = 1.64 \times 10^{21}$   $\text{cm}^{-3}$  and  $N_{\text{Er}} = 0.25 \times 10^{20}$   $\text{cm}^{-3}$ , the best fitted parameters are  $k = 3 \times 10^{-16}$   $\text{cm}^3/\text{s}$  and  $C_{\text{up}} = 1 \times 10^{-18}$   $\text{cm}^3/\text{s}$ , respectively, for the glass thickness of 0.5 mm. When the thickness of glass changes to 1.0 mm, the corresponding fitted parameters are  $k = 2.9 \times 10^{-16}$   $\text{cm}^3/\text{s}$  and  $C_{\text{up}} = 1 \times 10^{-18}$   $\text{cm}^3/\text{s}$ . The values of these parameters are different even if the doping concentrations are approximate. The value of  $k$  for our material is smaller than the upper boundary reported ( $5 \times 10^{-16}$   $\text{cm}^3/\text{s}$ ), but is larger than the values reported in other literatures. The value of  $C_{\text{up}}$  for  $\text{Er}^{3+}$  concentration is bigger than that reported in other literatures. The determination of  $k$  and  $C_{\text{up}}$  provides a good judgment for our  $\text{Yb}^{3+}/\text{Er}^{3+}$  codoped phosphate glass. Judging from the fitted parameters above, the characteristics of our glass could be further improved by increasing the value of  $k$  and reducing the value of  $C_{\text{up}}$ , which probably could be achieved by an optimization of the glass basics composition and doping concentration.

This work was supported by the International Cooperation Project of Shanghai Municipal Science and Technology Commission under Grant No. 05S207103.

## References

1. P. Laporta, S. Taccheo, S. Longhi, O. Svelto, and G. Sacchi, *Opt. Lett.* **18**, 1232 (1993).
2. P. Laporta, S. Taccheo, S. Longhi, O. Svelto, and C. Svelto, *Opt. Mater.* **11**, 269 (1999).
3. J. Zhou, F. Moshary, B. M. Gross, M. F. Arend, and S. A. Ahmed, *J. Appl. Phys.* **96**, 237 (2004).
4. F. Song, *Laser Optoelectron. Prog.* (in Chinese) **44**, (4) 15 (2007).
5. S. Taccheo, G. Sorbello, S. Longhi, and P. Laporta, *Opt. Quantum Electron.* **31**, 249 (1999).
6. M. Laroche, S. Girard, J. K. Sahu, W. A. Clarkson, and J. Nilsson, *J. Opt. Soc. Am. B* **23**, 195 (2006).
7. E. Tanguy, C. Larat, and J. P. Pocholle, *Opt. Commun.* **153**, 172 (1998).
8. G. C. Vally, *Opt. Fiber Technol.* **7**, 21 (2001).
9. B. Pedersen, B. A. Thompson, S. Zemon, W. J. Miniscalco, and T. Wei, *IEEE Photon. Technol. Lett.* **4**, 46 (1992).
10. J. Nilsson, P. Scheer, and B. Jaskorzynska, *IEEE Photon. Technol. Lett.* **6**, 383 (1994).
11. R. Francini, F. Giovenale, U. M. Grassano, P. Laporta, and S. Taccheo, *Opt. Mater.* **13**, 417 (2000).
12. R. Wu, J. D. Myers, M. J. Myers, and C. Rapp, *Proc. SPIE* **4968**, 11 (2003).
13. F. Song, S. Liu, Z. Wu, H. Cai, X. Zhang, L. Teng, and J. Tian, *J. Opt. Soc. Am. B* **24**, 2327 (2007).
14. F. Song, S. Liu, Z. Wu, H. Cai, J. Su, J. Tian, and J. Xu, *IEEE J. Quantum Electron.* **43**, 817 (2007).
15. V. L. Kalashnikov, V. G. Shcherbitsky, N. V. Kuleshov, S. Girard, and R. Moncorgé, *Appl. Phys. B* **75**, 35 (2002).
16. S. Taccheo, P. Laporta, S. Longhi, and C. Svelto, *Opt. Lett.* **20**, 889 (1995).